ELSEVIER

Coordination Chemistry Reviews
211 (2001) 255–278

COORDINATION CHEMISTRY REVIEWS

www.elsevier.com/locate/ccr

Quantitative photochemistry of organometallic complexes: insight to their photophysical and photoreactivity mechanisms

Alistair J. Lees *

Department of Chemistry, State University of New York at Binghamton, Binghamton, NY 13902-6016, USA

Received 22 March 1999; accepted 10 January 2000

Contents

Abstract

This review describes a recently developed photokinetic method for studying the quantitative photochemistry of systems where there are overlapping absorbances and inner filter effects at the excitation wavelength. The procedure has been applied to investigate the wavelength-dependent photochemistry of several organometallic complexes and, for each case, the results illustrate that the lowest-lying electronically excited states have different intrinsic reactivities. In each of the systems studied, the determined quantitative data has led

* Tel.: +1-607-7772362; fax: +1-607-7774478.
E-mail address: alees@binghamton.edu (A.J. Lees).

PII: S0010-8545(00)00283-6

to valuable new insight into their photophysical and photochemical mechanisms.

Keywords: Electronically excited states; Photophysical processes; Photochemical mechanisms; Transition metal organometallic compounds

1. Introduction

Quantitative determinations of photochemical events are essential to understanding many chemical steps [1–4]. When light is only absorbed by a single chromophore, it is a relatively simple matter to measure the amount of energy absorbed by that species [3]. However, when there are several absorbing species the situation becomes much more complicated. In these multicomponent cases, quantitative determinations can only be reached after accounting for inner filter effects [5].

Often, as a practical way of measuring a chemical reaction's quantum efficiency, inner filter absorbances can be minimized by only carrying out the reaction over a relatively small conversion [1–3]. Alternatively, the measurements may be simplified by changing the reaction conditions themselves. Usually, the greatest problems occur when the photoproduct species absorbs an increasing fraction of the light at the exciting wavelength during the course of the reaction. Such cases are common and the lack of an experimental method to accurately account for all the light absorbances in the system seriously compromises the quantitative determination.

There are several procedures that have been explored in fluorescence spectroscopy to account for inner filter absorbances. Once again, conventional methods have often been performed which seek to minimize inner filter effects rather than actually determine them [5]. In other approaches, though, cell-shift and cell-rotation techniques have been used to determine the intensity of the fluorescence from different parts of the solution within the cell [6–9]. Finally, the considerable advances in microelectronic detection have now made it feasible to obtain correction factors for inner filter absorbances based upon simultaneous fluorescence and absorbance measurements from the same solution [10].

Recent studies carried out in our laboratory have focused on determining the photophysical properties of organometallic complexes and the quantitative nature of their photochemical reactions. During the course of this work we have developed a kinetic procedure [11] for measuring photochemical quantum efficiencies in situations where there are several overlapping absorbances at the excitation wavelength. This procedure involves a mathematical treatment that takes into account the complicated inner filter effects in these photochemical transformations. In this way, we have been able to obtain the first quantitative measurements for a number of important organometallic reactions, some of which are pertinent to homogeneous catalysis. Significantly, in each of the cases we have studied, this approach has yielded valuable new insight to the photophysical and photochemical reaction mechanisms, particularly if the data are taken in conjunction with time-resolved

spectroscopic measurements. Herein, we review this kinetic method and describe results recently obtained for several organometallic systems.

2. Quantum efficiency measurements

A number of organometallic photochemical reactions are complicated by the fact that they often have several overlapping absorbances (reactant, product, and entering ligand) at the excitation wavelength. Consequently, our newly developed kinetic procedure [11] is ideally suited to study these multicomponent systems, as it is able to treat varying inner filter effects throughout the progress of a photochemical reaction. This method has been demonstrated to be an excellent one for the study of a wide range of organometallic photochemical transformations, including ligand substitution and intermolecular C–H and Si–H bond activation processes at transition metal centers where the reactant and product absorbances commonly overlap at the excitation wavelength. The procedure involves the determination of the quantum efficiency for a photochemical reaction (ϕ_{cr}), according to Eq. (1). Here, C_R is the concentration of the reactant species at various

$$\frac{-\mathrm{d}C_R}{\mathrm{d}t} = \phi_{cr} I_o (1 - 10^{-A_{tot}}) \frac{\varepsilon_R b C_R}{A_{tot}} \tag{1}$$

photolysis times t, I_o is the incident light intensity (in einsteins per unit time × solution volume), b is the cell pathlength and A_{tot} and ε_R are the total absorbance of the solution and molar absorptivity of the reactant species at the irradiation wavelength, respectively. Hence, Eq. (1) appropriately represents the quantum efficiency in terms of the change in concentration of the reactant species divided by the amount of the absorbed light that is due to the reactant in the presence of other absorbing species.

For a simple reaction where reactant (R) and product (P) are the only light absorbing species and C_R° is the concentration of R at $t = 0$, then:

$$A_{tot} = b[\varepsilon_R C_R + \varepsilon_P C_P] \tag{2}$$

and

$$C_P = C_R^\circ - C_R \tag{3}$$

thus

$$A_{tot} = b[(\varepsilon_R - \varepsilon_P) C_R + \varepsilon_P C_R^\circ] \tag{4}$$

For a reaction where an additional species (L) is present (such as excess ligand in photosubstitutional processes) then:

$$A_{tot} = b[\varepsilon_R C_R + \varepsilon_P C_P] + A_L \tag{5}$$

or

$$A_{tot} = b[(\varepsilon_R - \varepsilon_P) C_R + \varepsilon_P C_R^\circ] + A_L \tag{6}$$

For a reaction where the solvent (S) also absorbs at the irradiation wavelength then:

$$A_{tot} = b[\varepsilon_R C_R + \varepsilon_P C_P] + A_L + A_S \quad (7)$$

or

$$A_{tot} = b[(\varepsilon_R - \varepsilon_P)C_R + \varepsilon_P C_R^\circ] + A_L + A_S \quad (8)$$

Consequently, the variable A_{tot} in Eq. (1) represents the total absorbance ($A_{tot} = A_R + A_P + A_L + A_S$) at the excitation wavelength and the component ($\varepsilon_R b C_R / A_{tot}$) is the fraction of the absorbed light that is absorbed by the reactant species within the solution mixture at any point throughout the reaction. Thus, application of Eq. (1) accounts for the changing inner filter effects during the reaction caused by the varying light absorbances of the reactant, photoproduct and any additional species that are present.

Rearrangement and integration of Eq. (1) yields the following:

$$\mathrm{d} \ln C_R = -\phi_{cr} I_o \varepsilon_R b[(1 - 10^{-A_{tot}})/A_{tot}]\ \mathrm{d}t \quad (9)$$

and

$$\ln(C_R/C_R^\circ) = \alpha \int_{t_0}^{t_i} [(1 - 10^{-A_{tot}})/A_{tot}]\ \mathrm{d}t \quad (10)$$

where

$$\alpha = -\phi_{cr} I_o \varepsilon_R b \quad (11)$$

Our recent investigation of the photochemically-induced Si–H bond activation reaction of $CpRh(CO)_2$ [$Cp = \eta^5$-C_5H_5] in triethylsilane (Et_3SiH) (Eq. (12)) provides a representative example for the application of the above procedure [12]. UV–vis and FTIR spectra recorded during the course of this photochemical transformation are shown in Figs. 1 and 2. These spectral data are initially treated by plotting the variable $[(1 - 10^{-A_{tot}})/A_{tot}]$ against the irradiation time, where A_{tot} is the optical density at 458 nm; this graph is depicted in Fig. 3. The function $\int_{t_0}^{t_i}[(1 - 10^{-A_{tot}})/A_{tot}]\,\mathrm{d}t$ is subsequently obtained by determining the cumulative areas from this plot at the various times t. For ease of calculation, each individual segment of the function can be approximated to be that of a trapezoid [11]. It should be noted that in this silane activation reaction, A_L and A_S are negligible. In the analogous photosubstitution reactions with PR_3 ligands, the term A_L is usually significant [12,13].

$$CpRh(CO)_2 \xrightarrow[Et_3SiH]{h\nu,\ 485\ nm} CpRh(CO)(SiEt_3)H + CO \quad (12)$$

Thereafter, plots of $\ln[(A_t - A_\infty)/(A_o - A_\infty)]$ versus $\int_{t_0}^{t_i}[(1 - 10^{-A_{tot}})/A_{tot}]\,\mathrm{d}t$ are made, where A_o, A_t and A_∞ are absorbance values at any particular wavelength throughout the photolysis reaction. It should be recognized that the $\ln[(A_t - A_\infty)/(A_o - A_\infty)]$ values represent $\ln(C_R/C_R^\circ)$ in Eq. (10). These absorbance values can be taken from the UV–vis data, usually at an absorption maximum in the initial spectrum, but they can also be obtained from other spectroscopic data. In the case

of $CpRh(CO)_2$, the FTIR data of the carbonyl-stretching region display substantial absorbance changes (see Fig. 2) and it is preferable to use them.

Kinetic plots for the ν(CO) bands at 2046, 2009 and 1982 cm^{-1} are illustrated in Fig. 4. The parent complex is represented by the two decreasing infrared bands at 2046 and 1982 cm^{-1}, and it is observed that the kinetic plots are both linear and have coincident slopes α when $A_\infty = 0$. The photoproduct is represented by the increasing infrared band at 2009 cm^{-1}, and the kinetic plot displays a straight line when $A_\infty = 0.76$; an initial estimate of this value can be obtained from the spectral progression (see Fig. 2). Estimates of A_∞ that are either too high or low exhibit plots that deviate from linearity; this is especially pronounced in the later stages of photolysis (at high values of the integral function). Significantly, the slope α from this graph is coincident with the above determinations. These kinetic observations, in conjunction with a knowledge of the infrared spectrum of the product, illustrate that the reaction proceeds cleanly without interference from secondary photochemical or thermal processes and confirms the stoichiometry of this photochemical reaction (see Eq. (12)). Having found a mean value of $\alpha = 1.83(\pm 0.09) \times 10^{-3}$ from the above kinetic plots, it is then a straightforward matter to calculate ϕ_{cr} from Eq. (11) with the incident light intensity determined from the laser power or

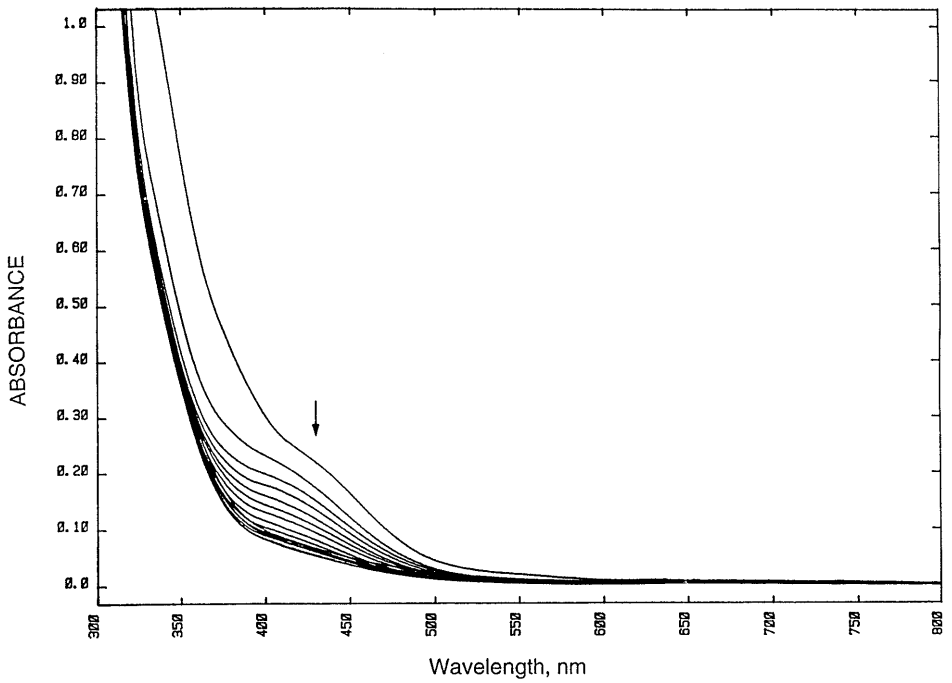

Fig. 1. UV–vis absorption spectral changes accompanying the 458-nm irradiation of 2.5 x 10^{-3} M $CpRh(CO)_2$ in deoxygenated decalin solution containing 0.1 M Et_3SiH at 298 K. Initial spectrum recorded prior to irradiation; subsequent spectra recorded after 30 min time intervals of irradiation. Reprinted, with permission, from Ref. [12].

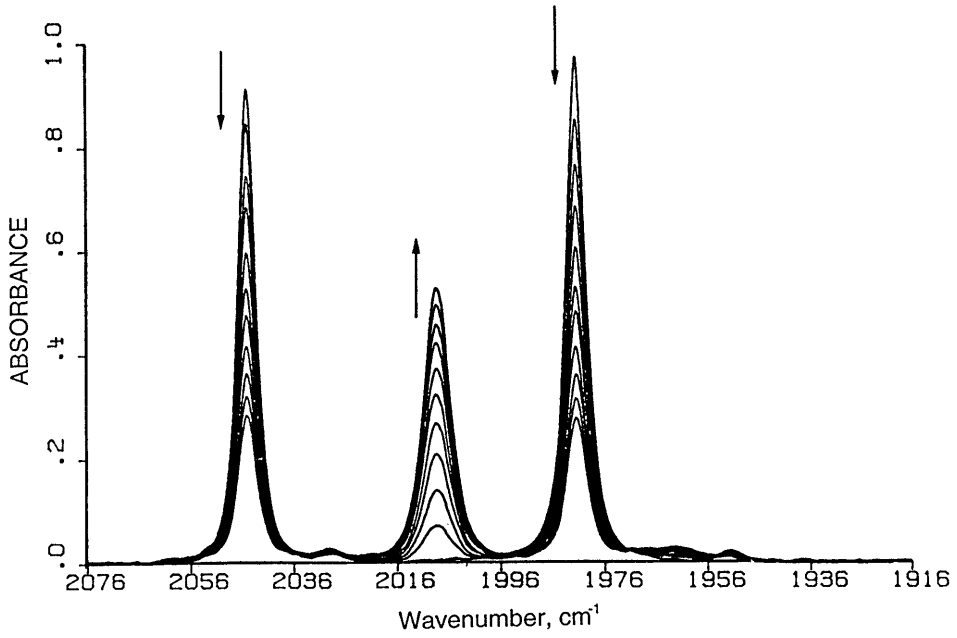

Fig. 2. FTIR absorption spectral changes accompanying the 458-nm irradiation of 2.5×10^{-3} M $CpRh(CO)_2$ in deoxygenated decalin solution containing 0.1 M Et_3SiH at 298 K. Initial spectrum recorded prior to irradiation; subsequent spectra recorded after 30 min time intervals of irradiation. Reprinted, with permission, from Ref. [12].

by actinometry. The above procedure is illustrated for $CpRh(CO)_2$, but it can be applied to the wide variety of organometallic photochemical processes which exhibit multicomponent absorbances at the excitation wavelength.

3. Organometallic systems

3.1. $CpRh(CO)_2$ and $Cp^*Rh(CO)_2$

Quantitative measurements have greatly facilitated an understanding of the photochemistry of the $CpRh(CO)_2$ and $Cp^*Rh(CO)_2$ [$Cp^* = \eta^5$-$C_5(CH_3)_5$] complexes [12–16]. Significantly, it was found that the quantum efficiencies for phosphine (PR_3) ligand substitution are wavelength dependent and influenced by both the entering ligand concentration and the nature of the entering ligand (see Figs. 5 and 6), implying that there are two excited states with distinct reactivities in the photochemical mechanism. Consequently, two different reaction intermediates are implicated in the solution photochemistry of $CpRh(CO)_2$ and $Cp^*Rh(CO)_2$. The photoreactivity was also studied in triethylsilane (Et_3SiH) solution and it can be seen that the quantum efficiencies are independent of entering Et_3SiH ligand concentration (see Fig. 5).

The photochemistry has been understood by invoking different pathways following excitation at short and long wavelengths. Upon 313-nm excitation (short wavelength) of $CpRh(CO)_2$ in hydrocarbon (RH) solution an upper-energy ligand field (LF) state is reached and the photoreactivity is characterized by facile CO dissociation and high quantum efficiency ($\phi_{cr} > 0.1$) for both ligand substitution and C–H/Si–H bond activation reactions (see Fig. 6) [13–16].

The photoefficiency data are entirely consistent with the primary photoproduct being the hydrocarbon solvated CpRh(CO) monocarbonyl species (see Scheme 1) [13–19]. However, it should be noted that the alkyl hydride complex, CpRh(CO)(R)H, is also unstable and has been identified as a reaction intermediate in flash photolysis; this transient species has a lifetime on the order of milliseconds in the absence of a scavenging ligand and it undergoes reductive elimination to form $[CpRh(\mu\text{-}CO)]_2$ and subsequently the *trans*-$Cp_2Rh_2(CO)_3$ product [20].

In sharp contrast, the 458-nm excitation (long wavelength) predominantly populates a lower-energy LF excited state which is characterized by an inefficient ($\phi_{cr} \sim 10^{-3}$) photosubstitution reaction (see Scheme 2). A ring slippage ($\eta^5 \rightarrow \eta^3$) mechanism involving the cyclopentadienyl ligand [21] has been postulated on the basis of the ϕ_{cr} results, which are influenced by the nature and concentration of the entering PR_3 ligand. In such a mechanism, the competition of a back ring-slip process effectively lowers the reaction quantum efficiency for photosubstitution. The (η^3-Cp)$Rh(CO)_2$ intermediate is once again considered to be solvated [15]. The photoreactivity at long wavelength, therefore, appears to be similar to the thermal substitutional chemistry of this system [22–26].

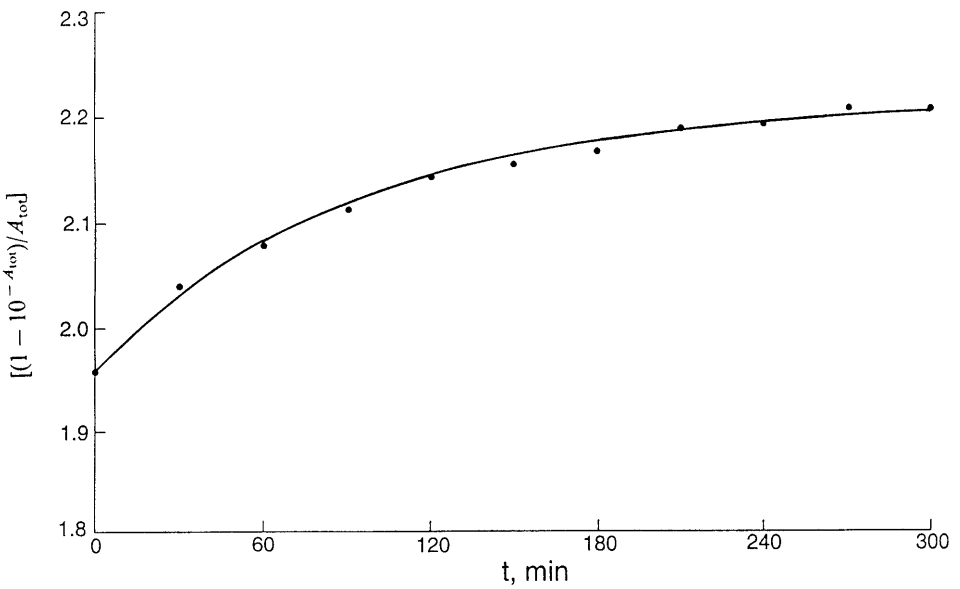

Fig. 3. Plot of the function $[(1-10^{-A_{tot}})/A_{tot}]$ versus time. Data taken from Fig. 1. Reprinted, with permission, from Ref. [11].

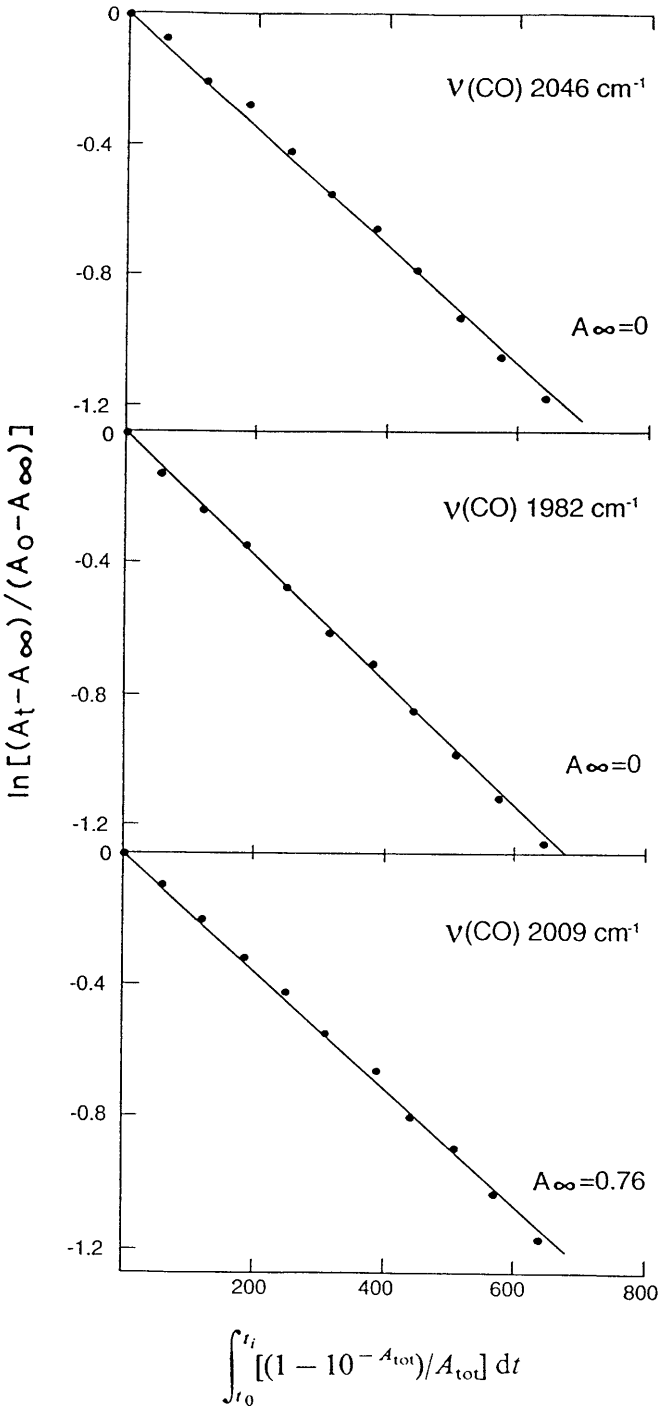

Fig. 4. Kinetic representations of the FTIR bands at 2046, 1982 and 2009 cm^{-1}. Reprinted, with permission, from Ref. [11].

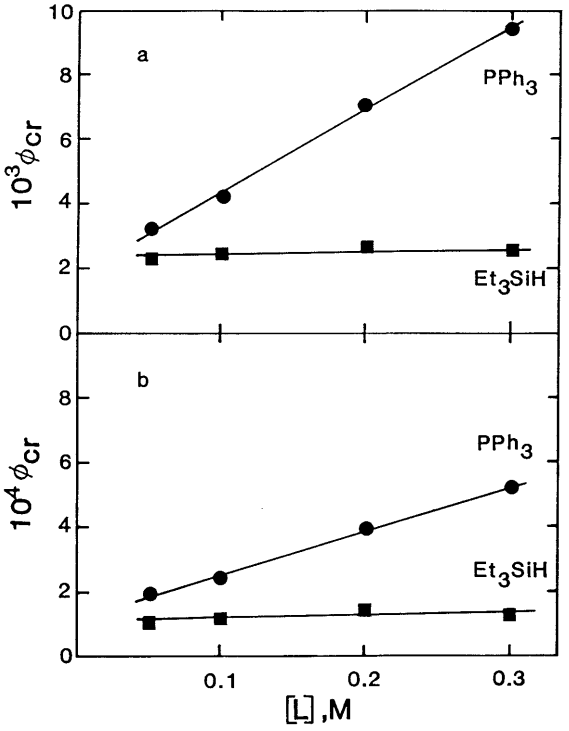

Fig. 5. Plots of photochemical quantum efficiencies (ϕ_{cr}) versus entering ligand (L) concentration for the reactions of (a) $CpRh(CO)_2$ and (b) $Cp^*Rh(CO)_2$ with PPh_3 and Et_3SiH. Excitation wavelength is 458 nm. Reaction with PPh_3 involves ligand substitution and reaction with Et_3SiH involves Si–H bond activation (Scheme 1). In (a) the photosubstitution data were obtained at 283 K and the Si–H bond activation data were recorded at 293 K. In (b) the data were obtained at 268 K. Each ϕ_{cr} value represents the mean of the least three readings; estimated uncertainties on ϕ_{cr} are within $\pm 5\%$. Reprinted, with permission, from Ref. [13].

In the absence of a scavenging PR_3 ligand and at low concentrations of Et_3SiH, photolysis at 458 nm results in competitive scavenging of the CpRh(CO) complex by CO and CpRh(CO), thereby providing a return route to the parent $CpRh(CO)_2$ complex or forming the bridged *trans*-$Cp_2Rh_2(CO)_3$ species [15]. Clearly, the CO dissociative process still occurs upon long-wavelength excitation, albeit less efficiently than photolysis at 313 nm. Photochemical quantum efficiencies at 458 nm for $CpRh(CO)_2$ in decalin under conditions of low concentration of added Et_3SiH exhibit saturation-type kinetics (see Fig. 7). The intercept point represents the quantum efficiency of the binucleation reaction alone. Importantly, when the binucleation reaction was measured under CO-saturated conditions, it was determined that no photochemical transformation took place at all. Under these kinetic conditions, CpRh(CO) is effectively scavenged by CO and the parent complex is generated again. At Et_3SiH concentrations above 0.4 M, it was found that there was no influence of added CO on the quantum efficiencies; under these conditions

all the CpRh(CO) molecules are scavenged by Et_3SiH. Kinetic analyses of all the photochemical pathways and their influence on the quantum efficiency have been previously described in detail [13,15].

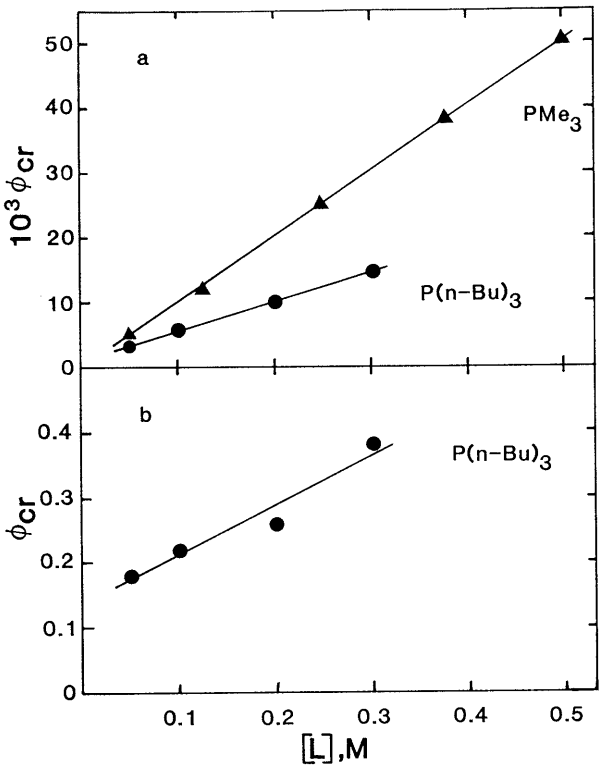

Fig. 6. Plots of photochemical quantum efficiencies (ϕ_{cr}) for the reaction of $CpRh(CO)_2$ with various concentrations of entering ligand, L = PMe_3 and $P(n\text{-}Bu)_3$, at 268 K. Excitation is at (a) 458 and (b) 313 nm. Each ϕ_{cr} value represents the mean of at least three readings; estimated uncertainties are within (a) $\pm$ 5% and (b) $\pm$ 10%. Reprinted, with permission, from Ref. [13].

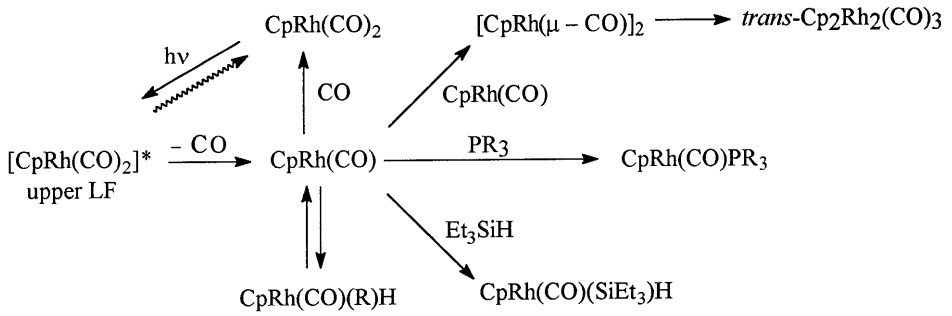

Scheme 1.

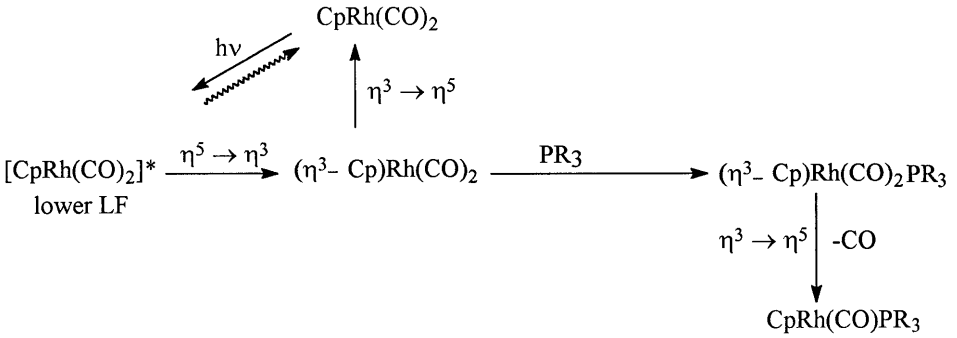

Scheme 2.

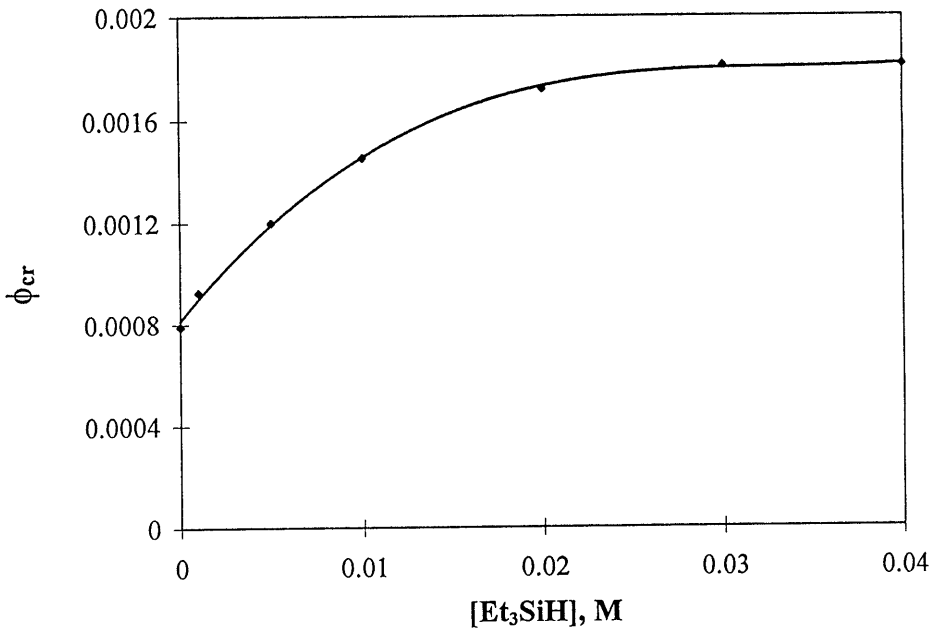

Fig. 7. Plots of photochemical quantum efficiency (ϕ_{cr}) versus Et_3SiH concentration for the 458-nm Si–H bond activation reaction of $CpRh(CO)_2$ in deoxygenated decalin at 293 K. Reprinted, with permission, from Ref. [15].

A key feature of the kinetic representation of the photochemistry is that the two LF excited states are extremely short lived, undergo rapid solvation, and then distinct chemical reactions occur (see Fig. 8) [15]. It is not that surprising that the photophysical processes are so fast; indeed CO dissociative reactions typically take place on the timescale of a few picoseconds [27–45], and the $CpRh(CO)_2$ and $Cp^*Rh(CO)_2$ complexes themselves have been shown to be non-luminescent at 77 K [13], consistent with rapid dissociations from LF states [46].

3.2. $(HBPz'_3)Rh(CO)_2$

Much attention has also been paid to understanding the photochemistry of the $(HBPz'_3)Rh(CO)_2$ (Pz′ = 3,5-dimethylolpyrazolyl) complex following the initial report of C–H activation [47]. Recently, we have studied the thermal and photochemical pathways in alkane solutions at room temperature [48,49]. The thermal mechanism has been characterized to involve rapid $\eta^3 \leftrightarrow \eta^2$ ligand interconversions and, indeed, the protonated complex, $[\{\eta^2\text{-}(HBPz'_3)(Pz'H)\}Rh(CO)_2]BF_4$, is readily formed on addition of $HBF_4{\cdot}OEt$ to $(HBPz'_3)Rh(CO)_2$. The photochemistry of $(HBPz'_3)Rh(CO)_2$ is exceptionally clean in each of the alkanes studied and conversion of the parent complex to form the hydrido photoproduct takes place completely (see Eq. (13)).

$$(HBPz'_3)Rh(CO)_2 \xrightarrow[RH]{h\nu} (HBPz'_3)Rh(CO)(R)H + CO \quad (13)$$

Absolute photochemical quantum efficiencies for intermolecular C–H bond activation (ϕ_{CH}) have been determined for these reactions and these show that the C–H activation process is strongly dependent on the exciting wavelength. Very effective conversion ($\phi_{CH} = 0.31$–0.34) is attained upon excitation at 313 or 366 nm (short wavelength) and inefficient conversion ($\phi_{CH} = 0.010$–0.011) is observed upon photolysis at 458 nm (long wavelength). The experimental observations have been again interpreted in terms of different photochemical mechanisms originating from two

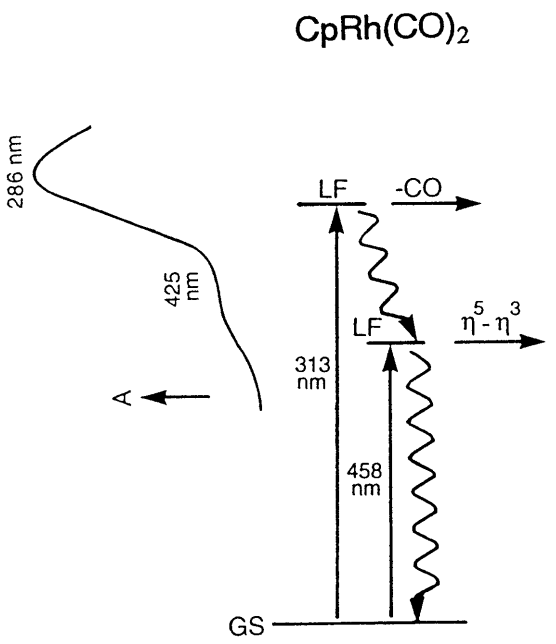

Fig. 8. Photophysical processes for $CpRh(CO)_2$ and $Cp^*Rh(CO)_2$ depicting distinct reactivities from two LF excited states. Reprinted, with permission, from Ref. [16].

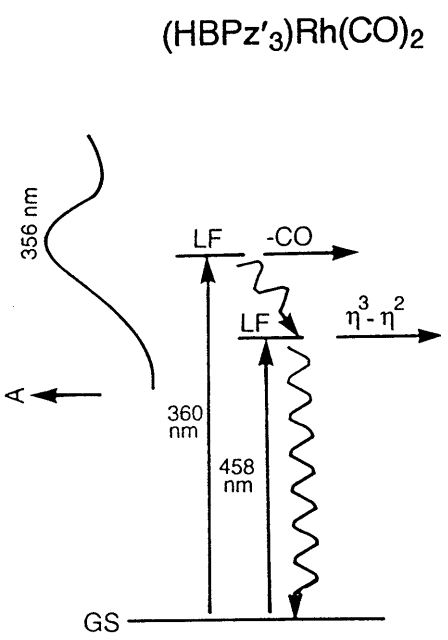

Fig. 9. Photophysical processes for $(HBPz'_3)Rh(CO)_2$ depicting distinct reactivities from two LF excited states. Reprinted, with permission, from Ref. [16].

low-lying LF states (see Fig. 9), in which the long-wavelength photochemistry and the thermal chemistry of $(HBPz'_3)Rh(CO)_2$ are associated with the initial formation of a solvated $(\eta^2\text{-}HBPz'_3)Rh(CO)_2$ intermediate that is unable to undergo C–H bond activation. The reduction in quantum efficiency is, thus, rationalized by an effective ligand rechelation ($\eta^2 \rightarrow \eta^3$) process of the η^2-intermediate. Significantly, we have prepared the analogous square planar $(H_2BPz_2)Rh(CO)_2$ complex (see below) and have found that it is reactive towards phosphine ligands but not R–H in room-temperature solution, supporting the conclusion that the above η^2-species is unable to C–H activate hydrocarbons.

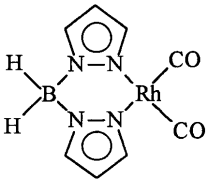

In sharp contrast, the short-wavelength photochemisty is attributed to proceed via an extremely short-lived monocarbonyl $(HBPz'_3)Rh(CO)$ complex that facilitates efficient C–H bond activation. Recent femtosecond flash photolysis measurements have confirmed that the primary photoproduct formed on UV excitation is indeed a monocarbonyl fragment which is produced and solvated within 10 ps [43].

Moreover, it has been determined that $(HBPz'_3)Rh(CO)_2$ is not luminescent in 2-Me-THF or EPA glasses at 77 K [48], consistent with LF levels which are highly dissociative and short lived [46]. Scheme 3 summarizes the postulated photochemical routes for the various excitation wavelengths on the basis of the quantum efficiency results [48,49].

Recently, the short-wavelength photochemistry of $(HBPz'_3)Rh(CO)_2$ has been investigated in further detail by ultrafast time-resolved infrared spectroscopy following excitation at 295 nm [50]. These experiments have elucidated several key events in the mechanism of the C–H bond activation reaction. Within a few ps after photoexcitation the alkane solvated monocarbonyl complex, $(HBPz'_3)Rh(CO)(R)H$, is formed as the first observable intermediate. This species subsequently undergoes $\eta^3 \rightarrow \eta^2$ ligand dechelation (200 ps) and then bond activation (230 ns) before $\eta^2 \rightarrow \eta^3$ ligand rechelation ($\ll 200$ ns) to form the activated photoproduct, $(HBPz'_3)Rh(CO)(R)H$. Clearly, the $\eta^3 \rightarrow \eta^2$ ligand dechelation step is an integral part of the C–H bond activation mechanism, even with short-wavelength excitation.

A comparison of the photophysical processes of the $CpRh(CO)_2$ and $(HBPz'_3)Rh(CO)_2$ complexes illustrates a number of similarities. As noted above, both molecules are believed to undergo extremely fast ligand dissociation reactions from LF excited states and, in each case, two different mechanisms involving CO dissociation and ligand interconversion are suggested. For $CpRh(CO)_2$, the electronic absorption spectrum indeed reveals two LF bands, but for $(HBPz'_3)Rh(CO)_2$ only a broad absorption is observed so the assignment of two excited states is less certain. In both cases the C–H activation photochemistry clearly arises by rapid CO dissociation and, yet, it is interesting to find that the observed ϕ_{CH} values are not dependent on added CO concentration [13,15,48,49]. Apparently, once the $(HBPz'_3)Rh(CO)$ primary photoproduct is formed it is not able to recombine with CO and it is converted completely to the C–H activated product. Hence, the photoefficiency of the C–H activation process appears to be determined solely by photophysical effects and, specifically, by the branching ratio between the dissociative and nondissociative pathways from the upper LF electronically excited state.

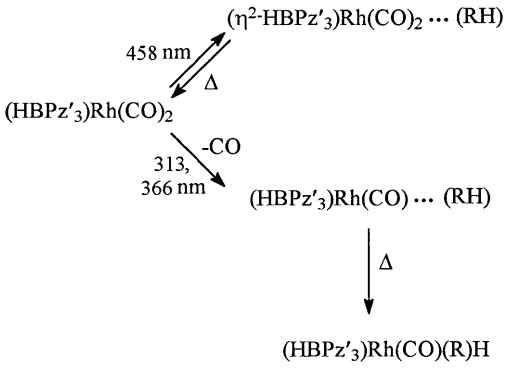

Scheme 3.

Table 1
Photochemical quantum efficiencies (ϕ_{cr}) as a function of excitation wavelength for the intermolecular Si–H bond activation reaction of $CpRh(CO)_2$ in deoxygenated hydrocarbon solutions at 293 K[a]

Solvent[b]	λ_{ex} (nm)		
	313	366	458
n-Hexane	0.29	0.078	0.0032
n-Heptane	0.29	0.060	0.0023
n-Octane	0.22	0.081	0.0026
Isooctane	0.31	0.089	0.0026
Decalin	0.15	0.060	0.0024
Benzene	0.035	0.017	0.00074
Benzene-d^6	0.054	0.024	0.00071
Toluene	0.036	0.0074	0.00082
p-Xylene	0.061	0.033	0.0014

[a] Data taken from Ref. [15]. Values were determined in triplicate and were reproducible to within ± 10%.
[b] Solutions contain 0.05 M Et_3SiH.

Table 2
Photochemical quantum efficiencies (ϕ_{CH}) for the intermolecular C–H bond activation reaction of $(HBPz'_3)Rh(CO)_2$ in deoxygenated hydrocarbon solutions at 293 K[a]

	λ_{ex} (nm)	ϕ_{CH}
Benzene	366	0.13
	458	0.0059
Toluene	366	0.14
	458	0.0073
p-Xylene	366	0.17
	458	0.0086
Mesitylene	366	0.22
	458	0.0092
n-Pentane	313	0.34
	366	0.32
	405	0.15
	458	0.011
n-Hexane	366	0.31
	458	0.011
n-Heptane	366	0.31
	458	0.010
Isooctane	366	0.31
	458	0.010

[a] Data taken from Refs. [48,49]. Values were determined in triplicate and were reproducible to within ± 8%.

Photoreactivity measurements on $CpRh(CO)_2$ and $(HBPz'_3)Rh(CO)_2$ have recently been carried out in several aromatic solutions at room temperature (see Tables 1 and 2) [15,48,49]. At any particular exciting wavelength, the photoeffi-

ciency values are similar across a range of alkanes but they are substantially reduced in aromatic solvents, even though it has also been determined that the aryl hydrido photoproducts are more thermodynamically stable than the alkyl hydrido species. The differences in quantum efficiency have been rationalized in terms of solvent effects on the nonradiative relaxation rates from the complexes, and more specifically from the upper LF levels responsible for the CO dissociative photochemistry. Hence, the main influence on the C–H activation photoefficiency is again attributed to photophysical effects in the different solvents [15,49].

3.3. $W(CO)_4(en)$

The $W(CO)_4(en)$ (en = ethylenediamine) complex has provided an excellent opportunity to study the photoreactivity of the lowest-lying LF absorption manifold at different exciting wavelengths [51]. This is because, unlike most substituted metal carbonyl complexes, the lowest-energy LF absorption band is removed from the other electronic transitions and the LF triplet is a distinctive feature of the spectrum (see Fig. 10). Consequently, in this system it is feasible to irradiate directly into the LF singlet and triplet levels separately and to measure the individual reactivities of these different states.

Quantitative measurements of the photochemistry of $W(CO)_4(en)$ in acetonitrile (see Eq. (14)) are shown in Table 3. Quantum efficiencies have been obtained

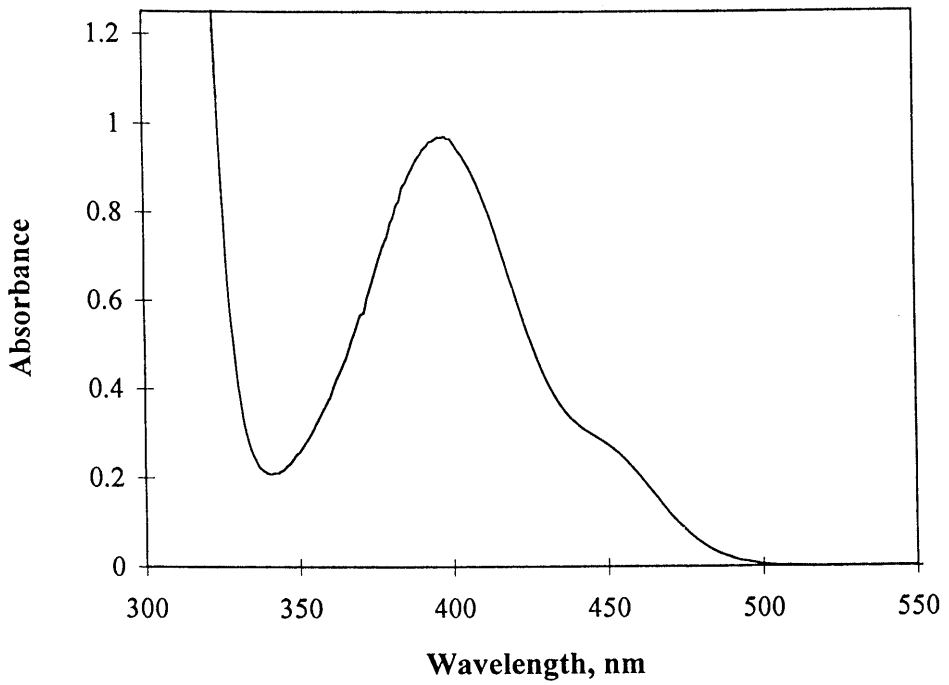

Fig. 10. Electronic absorption spectrum of $W(CO)_4(en)$ in acetonitrile at 293 K. Reprinted, with permission, from Ref. [51].

Table 3
Photochemical quantum efficiencies (ϕ_{cr}) for the CO ligand photosubstitution reaction of $W(CO)_4(en)$ in deoxygenated acetonitrile at 293 K[a]

λ_{ex} (nm)	ϕ_{cr}
313	0.23
366	0.068
405	0.050
458	0.007
476	0.007

[a] Data taken from Ref. [51]. Values were determined in triplicate and were reproducible to within ± 10%.

between 313 and 476 nm and these are strongly dependent on the excitation wavelength. Photolysis at 458 and 476 nm populates the lowest-energy LF triplet region and this results in significantly reduced photosubstitutional quantum efficiencies compared to photolysis at 366 or 405 nm which populates the corresponding LF singlet band. Furthermore, the observed quantum efficiency is even greater following excitation at 313 nm into a higher-energy LF level, demonstrating that this state undergoes CO dissociation with increased efficiency via an independent photophysical pathway.

$$W(CO)_4(en) \xrightarrow[CH_3CN]{h\nu} W(CO_3)(en)(CH_3CN) + CO \quad (14)$$

Clearly, the data for $W(CO)_4(en)$ reveal that the LF excited states undergo distinct photosubstitutional routes and that reaction from the lowest-lying LF triplet state occurs with substantially reduced photoefficiency. Similar behavior was reported for a series of pyridine (py) substituted *cis*-$W(CO)_4L_2$ (L = py, 4-Me-py, 4-Et-py) complexes which have LF transitions at lowest energy, although the distinct reactivities of the singlet and triplet states were not specifically addressed [52]. Moreover, the photosubstitutional quantum efficiencies of $W(CO)_5(py)$ and $W(CO)_5(pip)$ (pip = piperidine) have been found to be wavelength dependent, and again a reduced reactivity is observed from the lowest-lying triplet state [53,54]. In these latter molecules, the variations in the quantitative photochemistry have been associated with differences in the vibrational behavior of the participating excited states. The lowest-lying triplet LF level is understood to undergo substantial excited-state distortion in the form of a 'stretch' of the W–N bond [53–56], whereas the corresponding singlet LF level is thought to undergo a 'buckle' vibration [53,54,57–59]. The increased photoefficiency of the singlet state vibration may arise from this motion which exposes the metal center to solvating molecules on four faces of the octahedron. Certainly, solvent cage effects are anticipated to be quite different for the singlet and triplet LF energy levels in each of these systems.

3.4. $CpFe(CO)_2I$

A great deal has been learned about the photochemistry of the $CpFe(CO)_2I$ complex from studies of the quantitative photoreactivity at different excitation

wavelengths. Photolysis of the bromo and iodo derivatives in the presence of triphenylphosphine (PPh_3) leads to formation of the covalent species $CpFe(CO)(PPh_3)X$ (X = Br, I) with a high quantum efficiency ($\phi_{cr} = 0.14–0.89$) at 366 or 458 nm [60,61]. Furthermore, photolysis of $CpFe(CO)_2X$ (X = Cl, Br, I) in benzene solution saturated with ^{13}CO yields $CpFe(CO)(^{13}CO)X$ [61], and irradiations ($\lambda_{em} > 300$ nm) of $CpM(CO)_2Cl$ (M = Fe, Ru) in 12 K matrices have suggested that the principal reaction pathway involves CO dissociation and not M–Cl bond cleavage [62]. However, in other studies there is evidence indicating a heterolytic cleavage of the metal–halide bond [63–65], although the optimum photochemical conditions were not identified.

Recently, long-wavelength photolysis studies of $CpFe(CO)_2I$ have revealed that the iodide ligand can be effectively replaced by η^1-pyrrole ligands (pyrrole, indole) [66–69] or imidato ligands (cyclic imides, nucleobases, nucleosides) [70–72] in the presence of scavenging diisopropylamine (dipa) base. These reactions occur following excitation with either sunlight or a tungsten lamp. The absorption spectrum of $CpFe(CO)_2I$ illustrates only weak bands at long wavelength (see Fig. 11); however, we have found it is feasible to measure the quantitative photochemistry using a Kr^+ laser to perform excitation at 647 nm. The photochemical quantum efficiency for heterolytic cleavage at 647 nm has been determined to be 0.38 (± 0.02) [69]. This relatively high photoefficiency value is significant because it demonstrates that

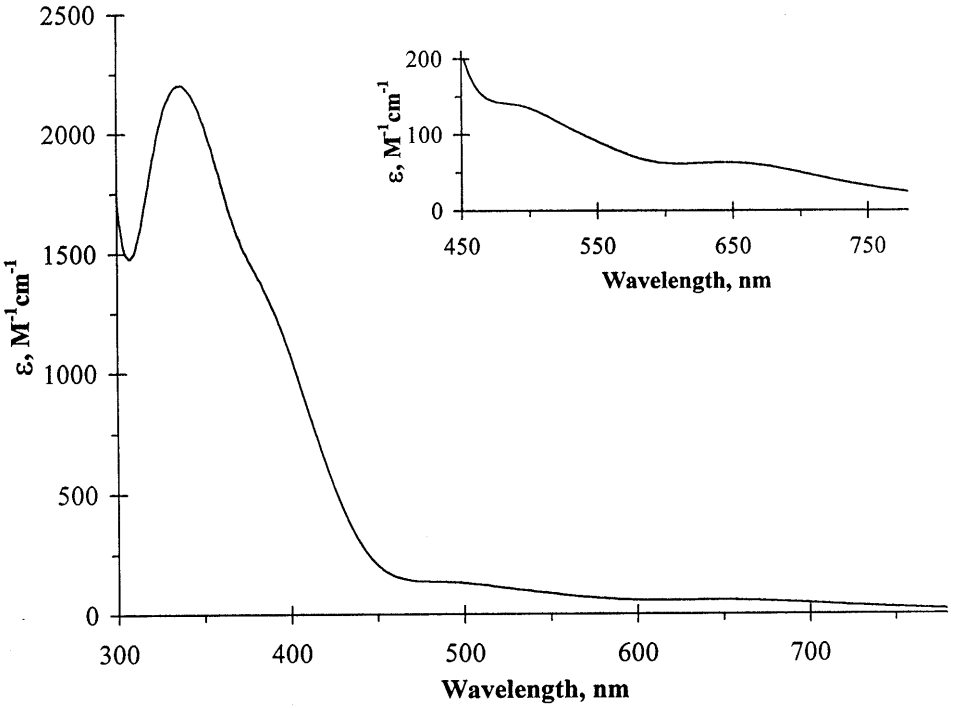

Fig. 11. Electronic absorption spectrum of $CpFe(CO)_2I$ in chloroform at 293 K. The inset depicts weak absorption bands at long wavelength. Reprinted, with permission, from Ref. [69].

irradiation at long wavelength can provide an effective route to new types of $CpFe(CO)_2L$ complexes which are, in turn, valuable precursors to azaferrocene. Such pathways are desirable because the metal center in azaferrocene has a greatly increased reactivity compared to that in ferrocene [73,74].

3.5. *[CpFe(η^6-ipb)]PF_6*

The [CpFe(η^6-arene)]X system is widely used in industry as a cationic photoinitiator in the polymerization of epoxides [75,76], dicyanate esters [77–79], pyrrole [80,81], styrene [82], dioxolenes [83] and acrylates [82,84,85]. One of these complexes, [CpFe(η^6-ipb)]PF_6 (ipb: isopropylbenzene), is frequently used in the manufacture of printed circuit boards [86–91] and in other coating applications [92]. The photochemical mechanism of [CpFe(η^6-ipb)]PF_6 is understood to involve an initial arene ring-slippage step prior to dissociation of the arene ligand [75,76,93–95]. Until recently, quantitative studies of the photochemistry have been confined to measurements at 436 nm. Here, light absorption populates the lowest-lying LF singlet excited state and it has been assumed that the intersystem crossing efficiency is unity and that the reactivity occurs entirely from the corresponding LF triplet level [93].

Recently, the photochemistry of [CpFe(η^6-ipb)]PF_6 has been studied over a range of excitation wavelengths [96]. Fig. 12 illustrates the UV–vis absorption spectrum of this complex and a typical spectral sequence observed on photolysis in the presence of 1,10-phenanthroline (phen) as scavenging ligand. Irradiations have been performed at 355, 458, 488, 514, 632 and 683 nm. Excitation in the 458–514 nm region results in population of the lowest-lying LF singlet state. Photolysis at 355 nm populates a higher-energy LF singlet state and may also involve some absorption into the long-wavelength tail of a higher-lying ligand-to-metal charge transfer (LMCT) band [97–99]. Irradiation at 632 and 683 nm directly populates the lowest LF triplet excited state, even though the absorbance band is very weak (in acetone, $\lambda_{max} = 650$ nm, $\varepsilon = 3.2\ M^{-1}cm^{-1}$). At each of the excitation wavelengths studied, the reaction involves conversion to the $[Fe(phen)_3]^{2+}$ photoproduct ($\lambda_{max} = 510$ nm), according to Eq. (15) [93,94].

$$[CpFe(\eta^6\text{-ipb})]PF_6 \xrightarrow[0.05\ M\ phen]{h\nu} [Fe(phen)_3]^{2+} + ipb + PF_6^- + Cp^- \quad (15)$$

Quantum efficiencies obtained for [CpFe(η^6-ipb)]PF_6 at various excitation wavelengths are shown in Table 4. Clearly, the ϕ_{cr} values exhibit a strong dependence on the excitation wavelength. The data reveal that the arene dissociation process takes place very effectively following excitation in the 355–514 nm region and population of either of the two lowest-lying LF singlet states. However, the reaction is much less efficient following long-wavelength excitation in the 632–683 nm region and direct population of the LF triplet level. Once again, the quantitative measurements reveal that in this molecule there are two excited states with differing intrinsic reactivities.

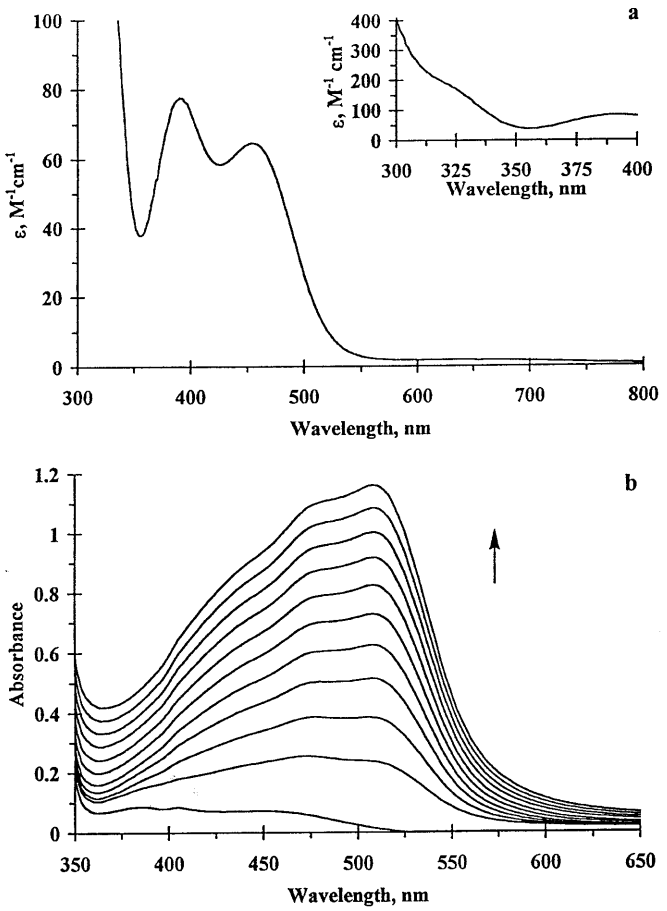

Fig. 12. (a) Electronic absorption spectra of [CpFe(η^6-ipb)]PF_6 in dichloromethane at 293 K. (b) UV–vis absorption spectral changes accompanying the 458-nm photolysis of 1×10^{-3} M [CpFe(η^6-ipb)]PF_6 in deoxygenated acetone containing 0.05 M phen at 293 K. Spectra are depicted following 1 min time intervals; initial spectrum was recorded prior to irradiation. Reprinted, with permission, from Ref. [96].

Table 4
Photochemical quantum efficiencies (ϕ_{cr}) for the arene dissociation reaction of [CpFe(η^6-ipb)]PF_6 in various solutions following excitation at several wavelengths[a]

Solvent	λ_{ex} (nm)					
	355 nm	458 nm	488 nm	514 nm	632 nm	683 nm
Acetonitrile	0.66(0.07)	0.64(0.01)	0.62(0.01)	0.49(0.007)	0.20(0.01)	0.15(0.002)
Acetone	0.61(0.03)	0.66(0.01)	0.65(0.01)	0.49(0.008)		0.14(0.004)
Nitromethane	[b]	0.72(0.01)	0.72(0.006)	0.55(0.003)		0.17(0.002)

[a] Data taken from Ref. [96]. Values in parenthesis represent the standard deviations from at least five measurements.
[b] Value was not obtained due to solvent absorption.

4. Concluding remarks

In each of the organometallic systems discussed, quantitative photochemical measurements have been able to provide considerable new insight to their photophysical and photochemical mechanisms. For the C–H activating $CpRh(CO)_2$, $Cp^*Rh(CO)_2$ and $(HBPz'_3)Rh(CO)_2$ molecules, the obtained quantum efficiencies have illustrated that there are two participating excited states that undergo quite different reaction mechanisms. For $W(CO)_4(en)$ and $[CpFe(\eta^6\text{-ipb})]PF_6$, the quantitative data reveal that the lowest-lying singlet and triplet excited states have distinct intrinsic reactivities and undergo separate photochemical routes to form their products. For $CpFe(CO)_2I$, an entirely different reaction pathway has been found following population of a low-lying reactive excited state.

Acknowledgements

We are grateful to the Division of Chemical Sciences, Office of Basic Energy Sciences, Office of Energy Research, US Department of Energy (Grant DE-FG02-89ER14039) for funding the author's research that is cited in this review.

Appendix A. Abbreviations

Cp	η^5-C_5H_5
Cp*	η^5-$C_5(CH_3)_5$
Dipa	diisopropylamine
En	ethylenediamine
EPA	ether–isopentane–ethanol (5:5:2 by volume)
FTIR	Fourier transform infrared
Ipb	isopropylbenzene
LF	ligand field
LMCT	ligand-to-metal charge transfer
MLCT	metal-to-ligand charge transfer
2-Me-THF	2-methyl-tetrahydrofuran
Phen	1,10-phenanthroline
Pz′	3,5-dimethylolpyrazolyl
UV	ultraviolet
Vis	visible
λ_{ex}	excitation wavelength
ϕ_{cr}	quantum efficiency of chemical reaction
ϕ_{CH}	quantum efficiency of C–H bond activation reaction

References

[1] J.G. Calvert, J.N. Pitts, Photochemistry, Wiley, New York, 1966.
[2] C.A. Parker, Photoluminescence of Solutions, Elsevier, Amsterdam, 1968.
[3] J.F. Rabek, Experimental Methods in Photochemistry and Photophysics, Wiley, New York, 1982.
[4] N.J. Turro, Modern Molecular Photochemistry, University Science Books, Mill Valley, CA, 1991.
[5] J.D. Ingle, S.R. Crouch, Spectrochemical Analysis, Prentice-Hall, Englewood Cliffs, NJ, 1988, p. 449.
[6] D.R. Christmann, S.R. Crouch, A. Timnick, Anal. Chem. 53 (1981) 276.
[7] D.R. Christmann, S.R. Crouch, A. Timnick, Anal. Chem. 53 (1981) 2040.
[8] K. Adamsons, A. Timnick, J.F. Holland, J.E. Sell, Anal. Chem. 54 (1982) 2186.
[9] K. Adamsons, J.E. Sell, J.F. Holland, A. Timnick, Am. Lab. 16 (1984) 16.
[10] M.C. Yappert, J.D. Ingle, Appl. Spectrosc. 43 (1989) 759.
[11] A.J. Lees, Anal. Chem. 68 (1996) 226.
[12] D.P. Drolet, A.J. Lees, J. Am. Chem. Soc. 112 (1990) 5878.
[13] D.P. Drolet, A.J. Lees, J. Am. Chem. Soc. 114 (1992) 4186.
[14] A.A. Purwoko, D.P. Drolet, A.J. Lees, J. Organomet. Chem. 504 (1995) 107.
[15] N. Dunwoody, A.J. Lees, Organometallics 16 (1997) 5770.
[16] A.J. Lees, J. Organomet. Chem. 554 (1998) 1.
[17] B.H. Weiller, E.P. Wasserman, C.B. Moore, R.G. Bergman, J. Am. Chem. Soc. 115 (1993) 4326.
[18] S.E. Bromberg, T. Lian, R.G. Bergman, C.B. Harris, J. Am. Chem. Soc. 118 (1996) 2069.
[19] C. Hall, R.N. Perutz, Chem. Rev. 96 (1996) 3125, and references therein.
[20] S.T. Belt, F.-W. Grevels, W.E. Koltzbücher, A. McCamley, R.N. Perutz, J. Am. Chem. Soc. 111 (1989) 8373.
[21] J.M. O'Connor, C.P. Casey, Chem. Rev. 87 (1987) 307.
[22] R. Cramer, L.P. Seilwell, J. Organomet. Chem. 92 (1975) 245.
[23] M.E. Rerek, F. Basolo, Organometallics 2 (1983) 372.
[24] M.E. Rerek, F. Basolo, J. Am. Chem. Soc. 106 (1984) 5908.
[25] L. Ji, M.E. Rerek, F. Basolo, Organometallics 3 (1984) 740.
[26] M. Cheong, F. Basolo, Organometallics 7 (1988) 2041.
[27] R. Bonneau, J.M. Kelly, J. Am. Chem. Soc. 102 (1980) 1220.
[28] A.J. Lees, A.W. Adamson, Inorg. Chem. 20 (1981) 4381.
[29] J.M. Kelly, C. Long, R. Bonneau, J. Phys. Chem. 87 (1983) 3344.
[30] J.D. Simon, X. Xie, J. Phys. Chem. 90 (1986) 6751.
[31] J.D. Simon, X. Xie, J. Phys. Chem. 91 (1987) 5538.
[32] J.D. Simon, X. Xie, J. Phys. Chem. 93 (1989) 291.
[33] L. Wang, X. Zhu, K.G. Spears, J. Am. Chem. Soc. 110 (1988) 8695.
[34] A.G. Joly, K.A. Nelson, J. Phys. Chem. 93 (1989) 2876.
[35] M. Lee, C.B. Harris, J. Am. Chem. Soc. 111 (1989) 8963.
[36] X. Xie, J.D. Simon, J. Am. Chem. Soc. 112 (1990) 1130.
[37] S.-C. Yu, X. Xu, R. Lingle, J.B. Hopkins, J. Am. Chem. Soc. 112 (1990) 3668.
[38] E. O'Driscoll, J.D. Simon, J. Am. Chem. Soc. 112 (1990) 6580.
[39] A.G. Joly, K.A. Nelson, Chem. Phys. 152 (1991) 69.
[40] T.P. Dougherty, E.J. Heilweil, J. Chem. Phys. 100 (1994) 4006.
[41] T.P. Dougherty, E.J. Heilweil, Chem. Phys. Letts. 227 (1994) 19.
[42] S.M. Arrivo, T.P. Dougherty, W.T. Grubbs, E.J. Heilweil, Chem. Phys. Letts. 235 (1995) 247.
[43] T. Lian, S.E. Bromberg, H. Yang, G. Proulx, R.G. Bergman, C.B. Harris, J. Am. Chem. Soc. 118 (1996) 3769.
[44] C.J. Arnold, T.-Q. Ye, R.N. Perutz, R.E. Hester, J.N. Moore, Chem. Phys. Letts. 248 (1996) 464.
[45] M.P. Wilms, E.J. Baerends, A. Rosa, D.J. Stufkens, Inorg. Chem. 36 (1997) 1541.
[46] A.J. Lees, Chem. Rev. 87 (1987) 711, and references therein.
[47] C.K. Ghosh, W.A.G. Graham, J. Am. Chem. Soc. 109 (1987) 4726.

[48] A.A. Purwoko, A.J. Lees, Inorg. Chem. 35 (1996) 675.
[49] A.A. Purwoko, S.D. Tibensky, A.J. Lees, Inorg. Chem. 35 (1996) 7049.
[50] S.E. Bromberg, H. Yang, M.C. Asplund, T. Lian, B.K. McNamara, K.T. Kotz, J.S. Yeston, M. Wilkens, H. Frei, R.G. Bergman, C.B. Harris, Science 278 (1997) 260.
[51] R.S. Panesar, N. Dunwoody, A.J. Lees, Inorg. Chem. 37 (1998) 1648.
[52] S. Chun, E.E. Getty, A.J. Lees, Inorg. Chem. 23 (1984) 2155.
[53] C. Moralejo, C.H. Langford, D.K. Sharma, Inorg. Chem. 28 (1989) 2205.
[54] C. Moralejo, C.H. Langford, Inorg. Chem. 30 (1991) 567.
[55] E.J. Heller, Acc. Chem. Res. 14 (1981) 368.
[56] L. Tutt, J.I. Zink, J. Am. Chem. Soc. 108 (1986) 5830.
[57] B.R. Hollebone, M.J. Stillman, J. Chem. Soc. Faraday Trans. 2 (1978) 2107.
[58] B.R. Hollebone, Theor. Chim. Acta 56 (1980) 45.
[59] B.R. Hollebone, C.H. Langford, N. Serpone, Coord. Chem. Rev. 39 (1981) 181.
[60] D.G. Alway, K.W. Barnett, Inorg. Chem. 17 (1978) 2826.
[61] D.G. Alway, K.W. Barnett, Adv. Chem. Ser. 168 (1978) 115.
[62] R.H. Hooker, K.A. Mahmoud, A.J. Rest, J. Chem. Soc. Dalton Trans. (1990) 1231.
[63] R.J. Haines, R.S. Nyholm, M.G.B. Stiddard, J. Chem. Soc. A (1968) 43.
[64] X. Pan, C.E. Philbin, M.P. Castellani, D.R. Tyler, Inorg. Chem. 27 (1988) 671.
[65] L.H. Ali, A. Cox, T.J. Kemp, J. Chem. Soc. Dalton Trans. (1973) 1475.
[66] J. Zakrzewski, J. Organomet. Chem. 327 (1987) C41.
[67] J. Zakrzewski, C. Giannotti, J. Organomet. Chem. 388 (1990) 175.
[68] J. Zakrzewski, J. Organomet. Chem. 412 (1991) C23.
[69] C.E. Borja, V. Jakúbek, A.J. Lees, Inorg. Chem. 37 (1998) 2281.
[70] J. Zakrzewski, J. Organomet. Chem. 359 (1989) 215.
[71] M. Bukowska-Strzyzewska, A. Tosik, D. Wódka, J. Zakrzewski, Polyhedron 13 (1994) 1689.
[72] J. Zakrzewski, A. Tosik, M. Bukowska-Strzyzewska, J. Organomet. Chem. 495 (1995) 83.
[73] D.L. Kershner, F. Basolo, Coord. Chem. Rev. 79 (1987) 279.
[74] J. Zakrzewski, C. Giannotti, Coord. Chem. Rev. 140 (1995) 169.
[75] K. Meier, H. Zweifl, J. Imaging Sci. 30 (1986) 174.
[76] K.M. Park, G.B. Schuster, J. Organomet. Chem. 402 (1991) 355.
[77] F.B. McCormick, K.A. Brown-Wensley, R. DeVoe, J. Polym. Mater. Sci. Eng. 66 (1992) 460.
[78] T.G. Kotch, A.J. Lees, S.J. Fuerniss, K.I. Papathomas, R. Snyder, Polym. Mater. Sci. Eng. 66 (1992) 462.
[79] T.G. Kotch, A.J. Lees, S.J. Fuerniss, K.I. Papathomas, Chem. Mater. 7 (1995) 801.
[80] J.F. Rabek, J. Lucki, M. Zuber, B.J. Qu, W.F. Shi, Polymer 33 (1992) 4838.
[81] J.F. Rabek, J. Lucki, M. Zuber, B.J. Qu, W.F. Shi, J. Macromol. Sci. Pure Appl. Chem. A29 (1992) 297.
[82] P. Wang, Y. Shen, S. Wu, E. Adamczak, L. Linden, J.F. Rabek, J. Macromol. Sci. Pure Appl. Chem. A32 (1995) 1973.
[83] C. Bolln, H. Frey, R. Muelhaupt, J. Polym. Sci. Part A: Polym. Chem. 33 (1995) 587.
[84] G. Eisele, J.P. Fouassier, R. Reeb, Angew. Makromol. Chem. 239 (1996) 169.
[85] N.S. Allen, M. Edge, A.R. Jasso, T. Corrales, M. Tellez-Rosas, J. Photochem. Photobiol. A 102 (1997) 253.
[86] A. Reiser, Photoreactive Polymers: The Science and Technology of Resists, Wiley-Interscience, New York, 1989.
[87] C. Kutal, C.G. Willson, Inf. Rec. Mater. 17 (1989) 373.
[88] R. Rubner, Adv. Mater. 2 (1990) 452.
[89] L.F. Thompson, C.G. Willson, S. Tagawa, Polymers for Microelectronics; ACS Symposium Series, vol. 537, ACS, Washington, DC, 1994.
[90] L.F. Thompson, C.G. Willson, M.J. Bowden (Eds.), Introduction to Microlithography, 2nd edition, ACS, Washington, DC, 1994.
[91] N. Bühler, D. Belluš, Pure Appl. Chem. 67 (1995) 25.
[92] N. Pietschmann, H. Schulz, Coating 29 (1996) 270.

[93] A.M. Nair, J.L. Schrenk, K.R. Mann, Inorg. Chem. 23 (1984) 2633.
[94] D.R. Chrisope, K.M. Park, G.B. Schuster, J. Am. Chem. Soc. 111 (1989) 6195.
[95] K.R. Mann, A.M. Blough, J.L. Schrenk, R.S. Koefod, D.A. Freedman, J.R. Matachek, Pure Appl. Chem. 67 (1995) 95, and references therein.
[96] V. Jakúbek, A.J. Lees, Chem. Commun. (1999) 1631.
[97] J.-R. Hanon, D. Astruc, P. Michaud, J. Am. Chem. Soc. 103 (1981) 758.
[98] M. Lacoste, H. Rabaa, D. Astruc, A. Le Beuze, J.-Y. Saillard, G. Précigoux, C. Courseille, N. Ardoin, W. Bowyer, Organometallics 8 (1989) 2233.
[99] G. Gamble, P.A. Grutsch, G. Ferraudi, C. Kutal, Inorg. Chim. Acta 247 (1996) 5.